

PAPER • OPEN ACCESS

Latest Results from NEMO-3 & Status of the SuperNEMO Experiment

To cite this article: David Waters and for the NEMO-3 and SuperNEMO Collaborations 2017 *J. Phys.: Conf. Ser.* **888** 012033

View the [article online](#) for updates and enhancements.

You may also like

- [Development of an optical simulation for the SuperNEMO calorimeter](#)
Arnaud Huber and on behalf of the SuperNEMO collaboration
- [The BiPo-3 detector for the measurement of ultra low natural radioactivities of thin materials](#)
A.S. Barabash, A. Basharina-Freshville, E. Birdsall et al.
- [Measurement of the distribution of \$^{207}\text{Bi}\$ depositions on calibration sources for SuperNEMO](#)
SuperNEMO Collaboration, R. Arnold, C. Augier et al.



ECS
The
Electrochemical
Society
Advancing solid state &
electrochemical science & technology

DISCOVER
how sustainability
intersects with
electrochemistry & solid
state science research

Latest Results from NEMO-3 & Status of the SuperNEMO Experiment

David Waters (for the NEMO-3 and SuperNEMO Collaborations)

Department of Physics & Astronomy, University College London, London WC1E 6BT, UK

E-mail: d.waters@ucl.ac.uk

Abstract. Neutrinoless double-beta decay is a uniquely sensitive probe of lepton number violating processes, and its observation may answer fundamental questions in neutrino physics, including the nature and the mass scale of the light neutrinos. Tracking calorimeter experiments have particular strengths, including the ability to search for neutrinoless double-beta decay amongst several different isotopes hosted in source foils. Full event reconstruction provides powerful background rejection capability, and the ability to disentangle different mechanisms for neutrinoless double-beta decay in the event of its discovery. These proceedings will give the latest results from the NEMO-3 experiment, including new double-beta decay measurements using the isotopes ^{48}Ca and ^{150}Nd . The current status and future prospects for the SuperNEMO experiment will also be presented.

1. Double-Beta Decay

The physics of double-beta decay and the motivation to search for neutrinoless double-beta decay ($0\nu\beta\beta$), is discussed in [1]. One of the motivations for NEMO-3 and subsequently SuperNEMO has been isotope *flexibility*, such that a putative signal can be confirmed in multiple isotopes. Moreover, the opportunity to measure standard-model decay modes such as 2-neutrino double beta decay ($2\nu\beta\beta$) to the ground state, as well as excited states, provides valuable tests of nuclear models.

1.1. The Tracker-Calorimeter Technique

NEMO-3 and SuperNEMO employ a tracker-calorimeter technique, depicted schematically in Figure 1 and further illustrated by means of a NEMO-3 double-beta candidate event in Figure 2. Double-beta decaying isotopes are hosted in thin foils surrounded by a tracking detector, which in turn is surrounded by a calorimeter. The great strength of this technique lies in its particle identification capability; α -particles can be identified as short, straight tracks, even without dE/dx information, and e^+/e^- discrimination is possible in an externally applied magnetic field. Unassociated calorimeter hits form γ candidates, although multiple Compton scatters make γ counting and energy reconstruction challenging. Timing information is also essential in such detectors, in order to reject particles of external origin through time-of-flight measurements, as well as to enable the identification of sequential decays, for example “BiPo” decays that occur in ^{238}U and ^{232}Th decay chains.

Full topological event reconstruction gives a very powerful means of rejecting backgrounds which do not have a 2-electron origin. In addition, opening angle and individual electron energy



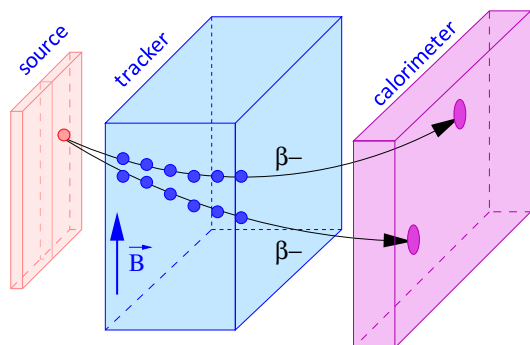


Figure 1. An illustration of the tracker-calorimeter technique, whereby the electrons from a double-beta decaying source traverse a tracking detector, before having their individual energies measured in a calorimeter.

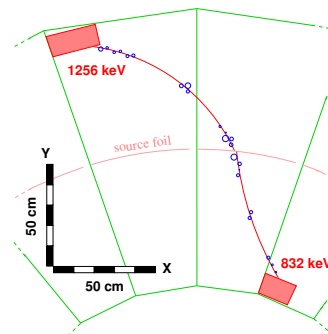


Figure 2. A NEMO-3 2-electron event in the search for $0\nu\beta\beta$ from ^{100}Mo . Two tracks have a common origin on the source foil, and project to separate energy deposits in the calorimeter (from [2]).

distributions can be used to disentangle different mechanisms behind neutrinoless double-beta decay in the event of a discovery.

2. The NEMO-3 Experiment

The NEMO-3 experiment ran from 2003 to 2011 in the Laboratoire Souterrain de Modane (LSM). It hosted 7 isotopes, with the largest masses comprised of ^{100}Mo (7 kg) and ^{82}Se (1 kg). 5-inch low radioactivity PMTs coupled to polystyrene scintillator blocks provided an energy resolution of $\Delta E(\text{FWHM})/E = 14\%/\sqrt{E(\text{MeV})}$. The tracking detector operated in Geiger mode with a low- Z gas mixture of 95% helium, 1% argon and 4% ethanol quencher. An external 25 Gauss magnetic field allowed the reconstruction of track curvature for e^+/e^- discrimination. Calibration systems, shielding and an anti-radon enclosure completed the detector structure.

2.1. Analysis Techniques

The results presented here arise from several separate analyses of NEMO-3 data. Although different in their details, all analyses exploit the full event reconstruction capability of NEMO-3 in order to constrain backgrounds in various control channels. Backgrounds originate from many sources, typically $\beta + \gamma$ decays where Compton scattering, Möller scattering or pair production can give rise to 2-electron topologies. Backgrounds originating from outside the detector are measured in samples selected with the characteristic time signature of a particle crossing the detector rather than originating in the source foil. One of the most important backgrounds, ^{214}Bi , can be measured in events containing 1 or more γ -rays in addition to a single electron, but also by looking for electron + α events with a time signature consistent with ^{214}Bi - ^{214}Po sequential decays. The spatial distribution of such events gives a further separation of this background into contributions internal to the source, and contributions likely to have arisen from the decay of ^{222}Rn inside the tracking volume. Another very important background from ^{208}Tl can be constrained, for example, by looking at the high γ -energy tail in $e + \gamma$ events.

Typically, the various background contributions are fitted simultaneously, or iteratively, in the different control samples. This gives rise to a highly constrained background prediction for the 2-electron channel, where the search for double-beta decay processes subsequently takes place.

3. Latest Results from NEMO-3

3.1. Final Results from ^{100}Mo .

NEMO-3 recently published the results of the search for $0\nu\beta\beta$ in ^{100}Mo with the full exposure of approximately $35 \text{ kg} \cdot \text{yr}$ [2, 3]. No signal is observed, and for the hypothesis of light-Majorana neutrino exchange, the following half-life limit is obtained :

$$T_{1/2}^{0\nu\beta\beta} > 1.1 \times 10^{24} \text{ yr (90\% C.L.) ,}$$

which corresponds to a limit on the effective Majorana neutrino mass $\langle m_\nu \rangle < 0.3 - 0.6 \text{ eV}$, where the range reflects nuclear matrix element (NME) uncertainties. This is the best half-life limit for the isotope ^{100}Mo and the limit on $\langle m_\nu \rangle$ is within a factor 2-3 of the best limits from other experiments, yet obtained with a much smaller isotope mass.

3.2. $2\nu\beta\beta$ measurements and $0\nu\beta\beta$ searches in ^{48}Ca and ^{150}Nd

^{48}Ca is a particularly interesting isotope in which to search for neutrinoless double-beta decay due to its high $Q_{\beta\beta}$ value of 4.3 MeV, putting the visible energy above almost all background processes. However it is difficult to enrich, and there is some theoretical evidence that it may have a relatively suppressed NME for $0\nu\beta\beta$. NEMO-3 has recently published its analysis of the small (7 g) sample it hosted (see Figures 3 and 4), obtaining the following measurement of the two-neutrino double-beta decay half-life :

$$T_{1/2}^{2\nu\beta\beta} = [6.4_{-0.6}^{+0.7}(\text{stat.})_{-0.9}^{+1.2}(\text{syst.})] \times 10^{19} \text{ yr .}$$

This result constitutes the most precise measurement of the two-neutrino half-life for ^{48}Ca and is in mild tension with nuclear shell model predictions of $\sim 4 \times 10^{19} \text{ yr}$ [4].

Another of the most promising isotopes in which to search for $0\nu\beta\beta$ is ^{150}Nd . It has a high $Q_{\beta\beta}$ value (3.4 MeV), as well as a favourable phase space factor for double-beta decay due to its large atomic number. NEMO-3 has recently published the final analysis of a 36.6 g sample of ^{150}Nd , obtaining a two-neutrino half-life in agreement with previous measurements :

$$T_{1/2}^{2\nu\beta\beta} = [9.34 \pm 0.22(\text{stat.})_{-0.60}^{+0.62}(\text{syst.})] \times 10^{18} \text{ yr .}$$

A new technique has been developed in the search for $0\nu\beta\beta$, using a ‘‘Boosted Decision Tree’’ (BDT) to exploit the full event reconstruction in order to optimise the signal and background separation [5]. Figure 5 shows an example of how variables other than the summed-energy offer good separation between backgrounds and different signal models, and Figure 6 shows the result of combining several such variables in a BDT. The result is a limit on the $0\nu\beta\beta$ half-life in ^{150}Nd of :

$$T_{1/2}^{0\nu\beta\beta} > 2.0 \times 10^{22} \text{ yr (90\% C.L.) ,}$$

corresponding to a limit on the effective Majorana neutrino mass $\langle m_\nu \rangle < 1.6 - 5.3 \text{ eV}$. The expected (observed) half-life limit is 11% (34%) better than obtained with the summed-energy distribution alone, proving the benefit of using multi-variate techniques in experiments such as NEMO-3 for which full topological event information is available [5].

3.3. Other NEMO-3 Analyses

Several other NEMO-3 analyses are currently underway and mentioned briefly here.

^{150}Nd is the best candidate isotope in which to search for neutrinoless quadruple-beta decay, a lepton-number violating process that can occur even if neutrinos are Dirac particles [6]. The NEMO-3 dataset is unique in its ability to explicitly identify such events, and the search for

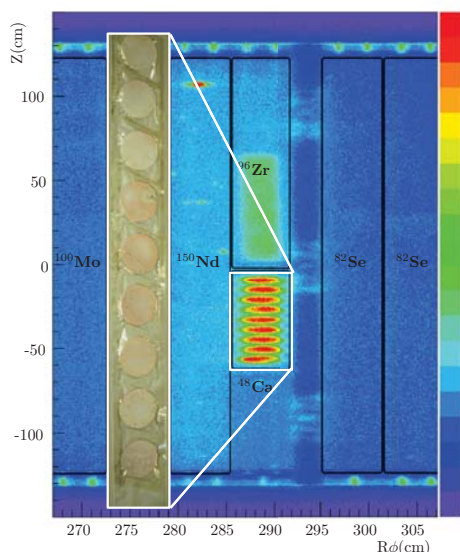


Figure 3. An image of the NEMO-3 source foils in the vicinity of the ^{48}Ca source, showing the relative rate of single-electron events from the nine CaF_2 disks (adapted from [4]).

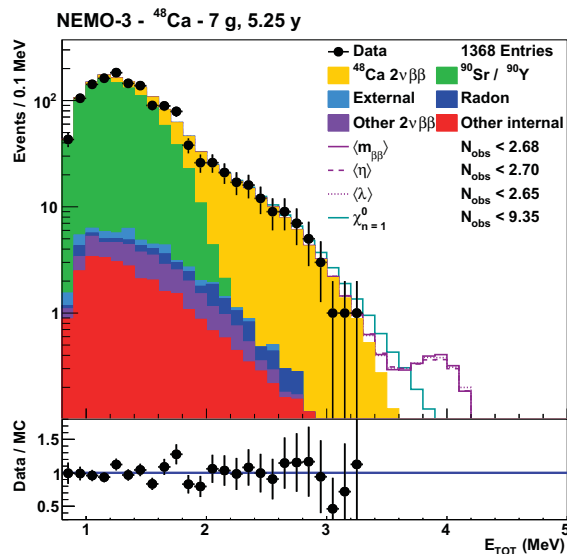


Figure 4. The distribution of the summed electron energy in 2-electron events in ^{48}Ca . The $2\nu\beta\beta$ -signal is clearly visible above backgrounds. Open histograms represent limits on non-standard model $0\nu\beta\beta$ processes. The ratio of data events to the total Monte Carlo prediction is shown in the bottom panel (from [4]).

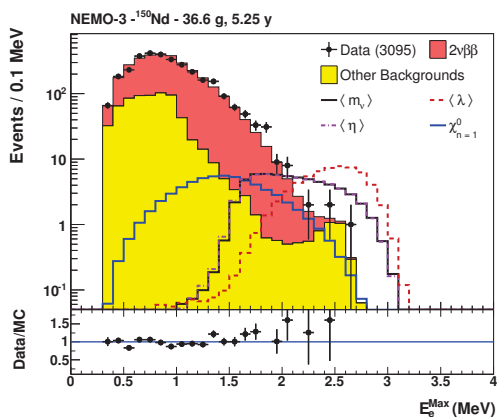


Figure 5. The maximum electron energy in 2-electron events from the analysis of ^{150}Nd . The different $0\nu\beta\beta$ -mechanisms all have a different shape from the $2\nu\beta\beta$ and other background processes. See [5] for details.

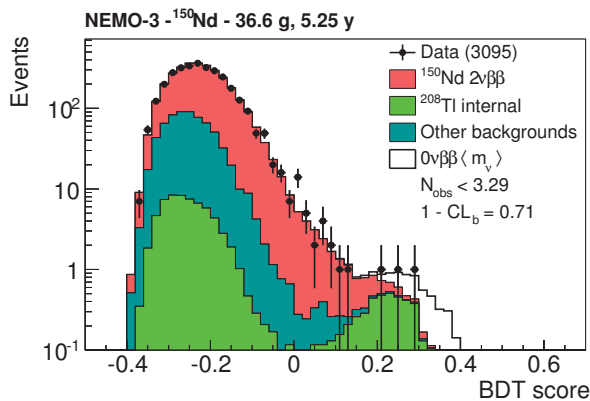


Figure 6. The Boosted Decision Tree (BDT) output, which combines 9 kinematic and detector parameters into a single score. The BDT provides better separation between backgrounds and (in open black histogram) $0\nu\beta\beta$ mediated by light-Majorana neutrino exchange. See [5] for details.

this process is currently underway. Figure 7 shows a 4-electron event in ^{100}Mo which, due to its larger mass and lack of $0\nu 4\beta$ decay mode, is an ideal sample in which to test the background

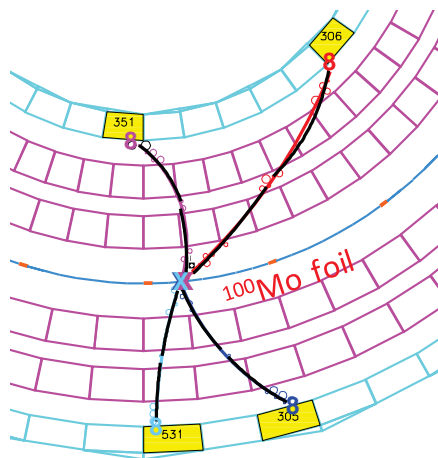


Figure 7. A 4-electron event originating from the ^{100}Mo foil in NEMO-3. This is a background control channel in the search for quadruple-beta decay in ^{150}Nd .

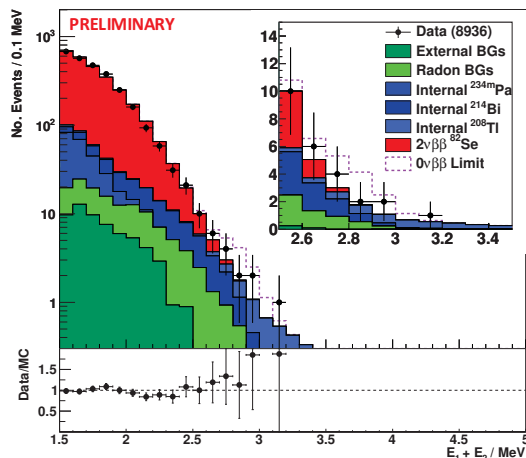


Figure 8. The distribution of the summed electron energy in 2-electron events in ^{82}Se . The shape of the $0\nu\beta\beta$ signal normalised to the 90% C.L. limit on the half-life, is indicated by the dashed open histogram.

modelling for this process.

NEMO-3 has recently released the final analysis of ^{116}Cd , providing the world's most precise measurement of the 2-neutrino half-life as well as a limit on the $0\nu\beta\beta$ half-life [7]. One particularly interesting aspect of this analysis is a test of the mechanism behind $2\nu\beta\beta$. It is found that single-state dominance (SSD) whereby 2-neutrino decay proceeds exclusively through the lowest-lying intermediate $J^\pi = 1^+$ state, is favoured over higher-state dominance (HSD) in which higher-energy intermediate 1^+ states are also involved.

The second largest-mass isotope hosted in NEMO-3 was ^{82}Se and it is especially important to make precise measurements of this, the baseline isotope for SuperNEMO. A preliminary final measurement of the $2\nu\beta\beta$ half-life has been performed :

$$T_{1/2}^{2\nu\beta\beta} = [10.07 \pm 0.14(\text{stat.}) \pm 0.54(\text{syst.})] \times 10^{19} \text{ yr} ,$$

which is more precise than the current world-average value. Figure 8 shows the region of interest in the summed-energy distribution for the $0\nu\beta\beta$ search. A half-life limit of 2.5×10^{23} yr (90% C.L.) is obtained, corresponding to $\langle m_\nu \rangle < 1.2 - 3.0$ eV, which is notable for being only 4 times worse than the half-life limit for ^{100}Mo yet obtained with only 15% of the isotope mass. The significantly longer $2\nu\beta\beta$ half-life is one of the important reasons for the better performance of ^{82}Se .

4. SuperNEMO

SuperNEMO is a successor to the NEMO-3 experiment, which at the 100 kg scale can start to probe neutrinoless double-beta decay half-lives of 10^{26} yr and Majorana mass scales down to ~ 50 meV. In order to achieve this, the energy resolution of the calorimeter needs to be improved by almost a factor of 2 and the radon background inside the tracker reduced by a factor of 30, with similarly large reductions in the internal background contaminations inside the source foil. A number of other technical improvements, for example to the calibration systems and stability monitoring, are being made. In the first phase a Demonstrator Module containing 7 kg of ^{82}Se , depicted in Figure 9, is in the final stages of construction.

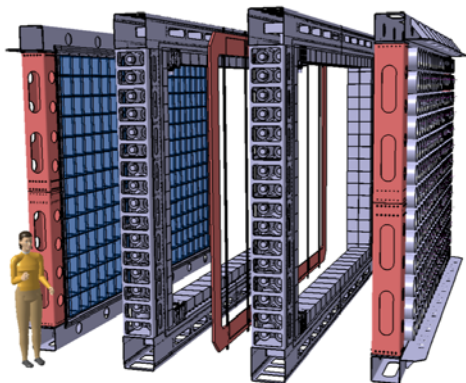


Figure 9. An exploded drawing of the SuperNEMO Demonstrator Module, showing the central source-foil frame (in red) sandwiched between two tracker modules, which are in turn sandwiched between the two calorimeter main walls.



Figure 10. A photograph of the coupling between the first tracker module and the first calorimeter main wall, which took place in October 2016 at the LSM. This completes the installation of half of the instrumented SuperNEMO Demonstrator Module detector.

4.1. SuperNEMO Status

The production of the calorimeter, employing 8-inch high-QE radio-pure PMTs coupled to polystyrene scintillator, is now complete, with the typical energy resolution meeting the requirements for SuperNEMO of 8%(FWHM) at 1 MeV. The production of the tracker modules, containing over 2000 individual Geiger cells, is also complete, and dedicated measurements indicate that radon activity levels at the required level of $150 \mu\text{Bq}/\text{m}^3$ can be achieved with reasonable gas-flow rates. In October 2016 the first half of the detector was integrated at LSM (see Figure 10) and the remaining parts of the detector will be added over the next 6 months, such that data-taking can commence in mid-2017.

5. Conclusions

NEMO-3 has been an extremely productive experiment, yielding competitive bounds on neutrinoless double-beta decay from ^{100}Mo , while at the same time producing a wealth of other measurements from the six other isotopes that it hosted. The SuperNEMO Demonstrator Module, which will have significantly better performance and lower backgrounds, is in an advanced stage of preparation at the LSM.

6. Acknowledgments

NEMO-3 and SuperNEMO have been made possible by the hard-work of the staff at the Modane Underground Laboratory. We acknowledge support by the grants agencies of the Czech Republic, CNRS/IN2P3 in France, RFBR in Russia, STFC in the U.K. and NSF in the U.S.

References

- [1] F. Deppisch, *these proceedings*.
- [2] R. Arnold *et al.*, Phys. Rev. D **89** (2014) 111101.
- [3] R. Arnold *et al.*, Phys. Rev. D **92** (2015) 072011.
- [4] R. Arnold *et al.*, Phys. Rev. D **93** (2016) 112008.
- [5] R. Arnold *et al.*, Phys. Rev. D **94** (2016) 072003.
- [6] J. Heeck and W. Rodejohann, Europhys. Lett. **103** (2013) 32001.
- [7] R. Arnold *et al.*, arXiv:1610.03226 [hep-ex].